Automated seed detection and three-dimensional reconstruction. II. Reconstruction of permanent prostate implants using simulated annealing

Dragan Tubic
Department of Radiation Oncology, Centre Hospitalier Universitaire de Québec and Centre de Recherche en Cancérologie de l'Université Laval, 11 Côte du Palais, Québeç G1R 2J6, Canada and Computer Vision and System Laboratory, Département de Génie Électrique et Genie Informatique, Université Laval, Québec G1K 7P4, Canada

André Zaccarin
Intel Corporation, 2200 Mission College Boulevard, Santa Clara, California 95052-8119

Luc Beaulieu
Department of Radiation Oncology, Centre Hospitalier Universitaire de Québec and Centre de Recherche en Cancérologie de l'Université Laval, 11 Côte du Palais, Québec GIR 2J6, Canada and Département de Physique, Université Laval, Québec G1K 7P4, Canada

Jean Pouliot
Department of Radiation Oncology, University of California, San Francisco, San Francisco, California 94143-1708

(Received 2 March 2001; accepted for publication 17 August 2001)

We present an algorithm, based on simulated annealing, for automatic seed matching and three-dimensional spatial coordinate reconstruction using either three radiographic films or three fluoroscopic images taken from different perspectives. The matching problem is defined in the framework of combinatorial optimization, which allows robust reconstruction in presence of calibration imprecision, patient movements, and isometric distortions. Furthermore, by using a global criterion to select the correct matching, we evade common problems of the three-film method and its variants in presence of noise. The algorithm has been tested on 112 clinical cases and 100 simulated implants and used clinically on more than 100 cases. Simulated implants were reconstructed with an average error of 0.21 mm. For clinical cases, comparison of the precision is performed between results obtained with this new method and results obtained using the three-film technique. Compared to the latter technique, the reconstruction precision was improved in 62% of the clinical cases. [DOI: 10.1118/1.1414309]

I. INTRODUCTION

As an important step of postimplant evaluation in brachytherapy, three-dimensional (3D) reconstruction of implants has received considerable attention during past 20 years. The best known and probably the most widely used method for 3D implant reconstruction has been the three-film method.[1–4] According to the reports in the literature[5] and our experience, this method does not provide an excellent precision: 90% of the seeds are reconstructed within 2 mm from their correct position. Approximately 8% of the seeds are reconstructed with errors greater than 5 mm, and some of the seeds are reconstructed with errors as big as 30 mm. Even if in some cases a small error is acceptable (2%–4% of the seeds), it is preferable to have a reconstruction as accurate as possible. In fact, some of our applications require 100% of the seeds to be reconstructed within 2 mm from their exact position.

Recently, a number of algorithms based on MRI or CT have been reported.[5–7] These algorithms suffer from ambiguities created by the space between consecutive images resulting in the number of detected seeds that can be twice as large as the number of implanted seeds. Also it is often the case that some of the seeds are connected on reconstructed images due to artifacts or insufficient resolution of the images. There is no overall validation criteria that can be used to indicate whether the reconstruction has been successful or not: A failure to correctly identify one of the seeds on the images leads immediately to a failure of correctly reconstructing that particular seed, and moreover, since the algorithms are often forced to reconstruct a specified number of seeds, one false seed also has to be inserted.

This paper presents a new method that aims at providing accurate and cost efficient procedure for 3D reconstruction of permanent implants using three sets of projections of seeds. The algorithm has been validated by reconstructing 100 implants generated by computer whose seed positions are known in advance. 112 clinical implants have also been reconstructed and the results were compared with the results previously obtained using the three-film method.

This new algorithm uses three sets of two-dimensional (2D) projections of seeds, which can be obtained either from radiographic films or fluoroscopic images. At our institution, fluoroscopic images were adopted since they are an inexpensive imaging modality, they do not require any film manipulation and, more importantly, they can be used to automatically extract 2D projections of the seeds. It is beyond the scope of this paper to describe the procedure of automated extraction of 2D projections and throughout this paper, it will be assumed that three sets of projections have already been

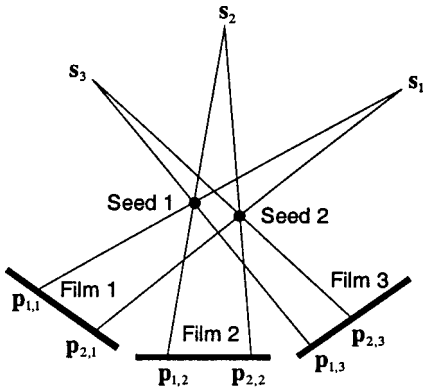

FIG. 1. Illustration of the matching problem.

acquired and properly placed in 3D space, according to the geometry of the simulator. A companion paper describes an algorithm for automatic seed localization.

II. METHODS

As for the three-film method, three films or three fluoroscopic images, taken from different perspectives, are used in order to obtain the three sets of projections that will be used to reconstruct the actual 3D positions of the seeds. A treatment simulator is used to acquire the images.

The real problem of the reconstruction is not obtaining the position of the seed but rather forming triplets of projections that will be used to reconstruct position for the seeds. This procedure will be referred to as matching. The matching problem is illustrated in Fig. 1.

For this simple case of two seeds, there are four possible solutions as shown in Table I. Since there is no way to know in advance which projections belong to which seed, the triplets of the projections have to be found before proceeding with the reconstruction. Due to an extremely large number of possible solutions, authors of three-film methods considered that it was impossible to verify all the combinations. This is due to the fact that in the early 1980s when these methods were developed, combinatorial optimization algorithms, such as simulated annealing, were unavailable or relatively unknown. The number of possible combinations of projections is $(N!)^2$ where N is the number of seeds. For an implant of 50 seeds there is 10^{128} possible solutions.

A common feature of all three-film techniques, and the main cause of its imprecision, is the use of a threshold to eliminate false solution. This approach, although very fast, can generate incorrect solutions as illustrated in Fig. 2.

There are two solutions equally plausible since the distance between the lines for both solutions is less than the threshold. When reducing the threshold there is the risk that some solutions could not be found due to the imprecision. To avoid this problem a global criterion is used to select the correct solution.

TABLE I. All possible solutions for matching the projections of two seeds.

	Solution 1	Solution 2	Solution 3	Solution 4
Seed 1	$\mathbf{p}_{1,1},\mathbf{p}_{1,2},\mathbf{p}_{1,3}$	$\mathbf{p}_{1,1},\mathbf{p}_{2,2},\mathbf{p}_{1,3}$	$\mathbf{p}_{1,1},\mathbf{p}_{1,2},\mathbf{p}_{2,3}$	$\mathbf{p}_{1,1},\mathbf{p}_{2,2},\mathbf{p}_{2,3}$
Seed 2	$\mathbf{p}_{2,1},\mathbf{p}_{2,2},\mathbf{p}_{2,3}$	$\mathbf{p}_{2,1},\mathbf{p}_{1,2},\mathbf{p}_{2,3}$	$\mathbf{p}_{2,1},\mathbf{p}_{2,2},\mathbf{p}_{1,3}$	$\mathbf{p}_{2,1},\mathbf{p}_{1,2},\mathbf{p}_{1,3}$

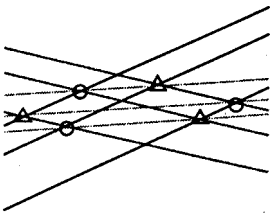

FIG. 2. Example of seed configurations that creates ambiguities undetectable by the three-film technique.

III. RECONSTRUCTION

Because of the intrinsic imprecision of the acquisition procedure, imaginary lines connecting x-ray source and the projections will never intersect perfectly and, therefore, it is possible to obtain only an approximation of the seed positions. The least-squares solution is used obtain the 3D seed position, as described in the following. Given M projections, $\mathbf{p}_1,\mathbf{p}_2,\ldots,\mathbf{p}_M$, obtained from M positions of the x-ray source, $\mathbf{s}_1,\mathbf{s}_2,\ldots\mathbf{s}_M$, the reconstructed position $\mathbf{p}^*$ of a seed is the point in 3D space for which the sum of its distance from the lines connecting the sources $\mathbf{s}_i$ to the projections $\mathbf{p}_i$ is minimum, i.e., $\mathbf{p}^*$ is the argument that minimizes the following function:

$$f(\mathbf{p}^*)=\sum_{i=1}^{M} d(L_i,\mathbf{p}^*), \tag{1}$$

where

$$d(L_i,\mathbf{p}^*)=\left\|\mathbf{p}^*-\mathbf{s}_i-\frac{(\mathbf{p}^*-s_i)^T(\mathbf{p}_i-\mathbf{s}_i)}{\mathbf{p}_i-\mathbf{s}_i}\right\|^2 \tag{2}$$

is the Euclidean distance between the point $\mathbf{p}^*$ and the line L_i. This distance will be referred to as the reconstruction error for the rest of the paper. Note that the reconstruction error is not the distance between the reconstructed and actual position of the seed. The line L_i connecting the x-ray source position $\mathbf{s}_i$ and the projection $\mathbf{p}_i$ is defined parametrically as

$$\mathbf{p}=\mathbf{s}_i+u\cdot(\mathbf{p}_i-\mathbf{s}_i). \tag{3}$$

It is easy to obtain the following result for the reconstructed seed position by deriving Eq. (1) with respect to $\mathbf{p}^*$. Given M projections of a seed, its reconstructed position $\mathbf{p}^*$ is

$$\mathbf{p}^*=\left[\sum_{k=1}^{M}\mathbf{A}_i\right]^{-1}\left[\sum_{k=1}^{M}\mathbf{A}_i\mathbf{p}_i\right], \tag{4}$$

$$\mathbf{A}_i=\mathbf{I}-\frac{(\mathbf{p}-\mathbf{s}_i)\cdot(\mathbf{p}_i-\mathbf{s}_i)^T}{\|\mathbf{p}_i-\mathbf{s}_i\|^2},\quad \mathbf{I}=\begin{bmatrix}1&0&0\\0&1&0\\0&0&1\end{bmatrix}. \tag{5}$$

IV. MATCHING

The matching problem can be formally stated as follows.

Let the matrix $\mathbf{P}=[\mathbf{p}_{ij}]$ of dimension $N\times M$ be a matrix whose elements $\mathbf{p}_{ij}$ are the coordinates of the projections of the seeds, where $i=1,...,N$ is the index of a projection on the film $j=1,...,M$. The initial order of the projections is the order in which the projections are entered in the computer and are considered as being completely random.

Definition 1: A solution of the matching problem is a matrix $\mathbf{\Pi}=[\pi_{ij}]$ whose column vectors $\boldsymbol{\pi}_j=(\pi_{1j},\pi_{2j},\ldots,\pi_{Nj})^T$ satisfy $\boldsymbol{\pi}_j\in\{$all permutations of $(1,2,...,N)\}$. The solution space Ω is defined as $\Omega=\{$all the matrices as defined in definition 1$\}$.

Cost function $f:\Omega\rightarrow\Re$ is defined as

$$f(\mathbf{\Pi})=\sum_{i=1}^{N}\sum_{j=1}^{M}\|d(L_{\pi_{ij}j},\mathbf{p}_i^*)\|^2, \tag{6}$$

where $L_{\pi_{ij}j}:\mathbf{p}=\mathbf{s}_j+u\cdot(\mathbf{p}_{\pi_{ij}j}-\mathbf{s}_j)$. The cost function represents the sum of reconstruction errors for all reconstructed seeds. The optimal solution is a solution $\mathbf{\Pi}^*\in\Omega$ such that

$$f(\mathbf{\Pi}^*)\leqslant f(\mathbf{\Pi}),\forall\mathbf{\Pi}\in\Omega. \tag{7}$$

A solution $\mathbf{\Pi}$ of the matching problem is a matrix of indices specifying which projections will be used to reconstruct each seed; e.g., the seed i will be reconstructed using the projections $\mathbf{p}_{\pi_{i1}1}$, $\mathbf{p}_{\pi_{i2}2}$, and $\mathbf{p}_{\pi_{i3}3}$. For example, in Table I, the matrix $\mathbf{\Pi}$ that corresponds to solution (3) is

$$\mathbf{\Pi}=\begin{pmatrix}1&1&2\\2&2&1\end{pmatrix}.$$

In other words, we want to find the solution that best approximates the actual implant using measured projections. Note that finding the minimum of this cost function does not imply that each seed will be reconstructed with the minimal reconstruction error.

The optimal solution, which minimizes the cost function Eq. (6) can be obtained using a combinatorial optimization algorithm. Simulated annealing proposed by Kirkpatrick *et al.*[8,9] was chosen for that purpose. Simulated annealing is a well-known algorithm successfully applied on a variety of combinatorial optimization problems. The detailed description of the algorithm is out of the scope of this paper, but can be found in Refs. 8 and 9. The general functioning of the algorithm is given in the following:[8] (1) initialize control parameter c_0, initial configuration Π_0, and the sequence length L_0. Set $k=0$ (number of the iterations); (2) generate a new configuration Π_{k+1}; (3) if $f(\Pi_{k+1})\leqslant f(\Pi_k)$ the change is accepted. If not the change is accepted with the probability

$$\exp\left(\frac{f(\Pi_{k+1})-f(\Pi_k)}{c_k}\right);$$

(4) repeat steps (2) and (3) L_k times; (5) $k\leftarrow k+1$, calculate new values for L_k and c_k; (6) repeat steps (2)–(5) until some stopping criteria is satisfied.

The parameters of the algorithm are a compromise between the speed of the execution and the quality of the solution found: By increasing the algorithm's speed, the probability that the algorithm will end up finding a local minimum rather than the global one is also increased. 100 implants were generated with known seed positions and the simulated annealing parameters were adjusted until all the implants were reconstructed correctly. The parameters are specified as follows:

(a) initial "temperature" c_0 was found by "melting" the system until most of the proposed reconfiguration were accepted (95%);
(b) initial configuration is random;
(c) sequence length L_k is fixed—steps (2) and (3) are repeated until the number of accepted reconfigurations is greater or equal to $10\times$number of seeds or the number of rejected reconfigurations is greater or equal to $100\times$ number of seeds;
(d) the temperature is decreased using the following cooling schedule—$c_k=c_0/(1+k^*\alpha)$, where $\alpha=3.5$;
(e) the algorithm stops when the temperature decreases below 0.5.

Two different types of reconfigurations were used. For the first type of reconfiguration, two randomly chosen projections belonging to the same, randomly chosen, film are exchanged. In other words $\pi_{i,k}$ and $\pi_{j,k}$ are exchanged, where $i,j\in[0,N)$ and $k\in[0,M)$ are randomly chosen. This type of reconfiguration is made with probability 0.9. The second type of reconfiguration forces the algorithm to explore different regions of the search space. This type of reconfiguration corresponds to a random reordering of all projections $\pi_{l,k}$, $l,k\in[i,j]$ and $k\in[0,M),i\leqslant j$, where i and j are also randomly chosen. The probability of this type of reconfiguration is 0.1.

At low temperatures simulated annealing becomes an inefficient local search algorithm, since most of the proposed reconfigurations will lead to an increase of the cost function and will therefore be rejected. It is possible to improve the execution time of the algorithm by stopping the simulated annealing at some point and use a local search algorithm. Empirically, it is found that if the simulated annealing is stopped when the temperature falls below 0.5, the solution will be good enough so that a local search can be performed to find the global minimum. The local search corresponds to the first type of reconfiguration as described previously but the projections are not chosen randomly: All $\pi_{i,k}$ and $\pi_{j,k}$, $i,j\in[0,N)$ and $k\in[0,M)$ were exchanged until no further improvement is possible.

The execution time of the algorithm can be shortened if the reconstruction errors [see the cost function of Eq. (1)] for all the triplets of projections are precomputed. This way, during the execution of the algorithm, the cost function [Eq. (6)] can be calculated simply by reading and adding the appropriate values from a table. Note that the number of triplets is not the same as the number of possible solutions. The number of possible triplets is N^3. Although additional time is

required to calculate the table, the performance improvement is large since the number of evaluations of the cost function is usually much larger than N^3. The quality of the solution depends on the quality of the random number sequences, and one needs to ensure that the specific algorithm of the random number generator will have a very large period. Excellent results were obtained with *Mersenne Twister* generator[10] whose period is $2^{19\,937}-1$ and gives uniform distribution up to 623 dimensions.

V. CORRECTION OF TRANSLATIONS AND ROTATIONS

Patient movements, hardware imprecision, and operator errors might affect the precision of the measured projections. These kinds of imprecisions will be referred to as distortions for the rest of the paper. Most of them, however, are isometric and the resulting image is a perfect image of the seed cloud at the moment of the acquisition, although taken from an unknown perspective. Therefore, there has to be such transformation that will put the image planes and the x-ray source positions so that lines connecting the projections and the x-ray source intersect perfectly. It is assumed that the prostate does not change shape between two consecutive images and that the projections have been found correctly. To correct the distortions, the same cost function as defined in Eq. (6) is minimized, but this time with respect to rotation angles and translation vectors. If the initial conditions, i.e., measured distances and angles, are close enough to their exact values, a strictly local search will end up very close to the desired minimum. It is however possible that, if the rotations and translations are corrected simultaneously, the correct implant does not correspond to a minimum of the cost function, which might result in scaling the seed cloud. To avoid this problem, correction of rotations and translations are separated.

To preserve the absolute orientation of the implant, one of the images is always kept fixed and the positions of the others are estimated. In other words the following function is minimized with respect to angles α_j, β_j, and γ_j:

$$\underset{\substack{\alpha_j,\beta_j,\gamma_j \\ j\in[1,M],j\neq k}}{\operatorname{argmin}} \; f(\Pi)=\sum_{i=1}^{N}\sum_{j=1}^{M}\|d(L_{\pi_{ij}j},\mathbf{p}_i^*)\|^2, \tag{8}$$

where M is number of films, k is index of the film that is kept fixed, and $\alpha_k=\beta_k=\gamma_k=0$. The lines connecting projections and x-ray sources are defined as

$$L_{ij}:\mathbf{p}=\mathbf{s}_j'+u\cdot(\mathbf{p}_{ij}'-\mathbf{s}_j'), \tag{9}$$

where the rotated projections $\mathbf{p}_{ij}'$ and x-ray sources $\mathbf{s}_j'$ are given by

$$\mathbf{p}_{ij}'=\mathbf{R}_x(\alpha_j)\mathbf{R}_y(\beta_j)\mathbf{R}_z(\gamma_j)\mathbf{p}_{ij}, \tag{10}$$

$$\mathbf{s}_j'=\mathbf{R}_x(\alpha_j)\mathbf{R}_y(\beta_j)\mathbf{R}_z(\gamma_j)\mathbf{s}_j. \tag{11}$$

The rotation matrices $\mathbf{R}_x$, $\mathbf{R}_y$, and $\mathbf{R}_z$ are defined as

$$\mathbf{R}_x(\alpha_j)=\begin{bmatrix}1 & 0 & 0\\ 0 & \cos(\alpha_j) & -\sin(\alpha_j)\\ 0 & \sin(\alpha_j) & \cos(\alpha_j)\end{bmatrix},$$

$$\mathbf{R}_y(\beta_j)=\begin{bmatrix}\cos(\beta_j) & 0 & \sin(\beta_j)\\ 0 & 1 & 0\\ -\sin(\beta_j) & 0 & \cos(\beta_j)\end{bmatrix}, \tag{12}$$

$$\mathbf{R}_z(\gamma_j)=\begin{bmatrix}\cos(\gamma_j) & -\sin(\gamma_j) & 0\\ \sin(\gamma_j) & \cos(\gamma_j) & 0\\ 0 & 0 & 1\end{bmatrix}.$$

The correct implant corresponds to a global minimum of this cost function, and this minimum can be found using a local search algorithm if the initial conditions $\alpha_j=\beta_j=\gamma_j=0$ correspond to a point in the same valley as the global minimum. Practically, this means that the distortions have to be relatively small: Experimentally, it is found that angular errors up to 10° can be corrected. However it is recommended to keep these errors in the interval $(-2.5, 2.5)$, which is usually sufficient for all practical purposes.

Since the x rays are approximately parallel in close vicinity of the iso-center, it is possible to show that small translations of the implant will not affect the shape of the reconstructed implant. Assuming that the projections are correctly matched and that the orientation was well estimated, the translation of the implant during acquisition can be detected by minimizing the following function:

$$\underset{\substack{\boldsymbol{\epsilon}_j \\ j\in[1,M]}}{\operatorname{argmin}} \; f(\Pi)=\sum_{i=1}^{N}\sum_{j=1}^{M}\|d(L_{\pi_{ij}j},\mathbf{p}_i^*+\boldsymbol{\epsilon}_j)\|^2, \tag{13}$$

where $\boldsymbol{\epsilon}_j=[x_T \quad y_T \quad z_T]^T$ is a translation vector.

Since it is the seeds and not the image planes that are translated, it is guaranteed that the size of the seed cloud will be preserved. To minimize the above-mentioned functions Brent's Praxis algorithm[11] was used.

Until now it was assumed that the projections were correctly matched, that 2D projections were perfectly extracted, and that the orientation of the implant was correctly estimated as described previously. In reality it is hardly the case. The matching algorithm, however, is robust enough to correctly match most of the projections in presence of distortions as large as rotations of 10° or translations of a few millimeters. We estimate that the matching is good enough so that distortions can be corrected or at least their influences reduced. Also, correction of distortions depends on quality of matching.

In other words, the success of the correction depends on the quality of the matching, and vice versa. To solve this problem the matching and corrections are iterated until no further improvement is possible. The overall procedure is summarized as follows:

(1) match the projections,
(2) for $k=0,1,2$ repeat steps (3) and (4),

(3) fix the film k and correct rotations,
(4) correct translations,
(5) repeat until no further improvement is possible.

VI. VALIDATION OF THE RECONSTRUCTION

It was shown that a fixed threshold could not always be used to match the projections correctly, especially in the presence of distortions. However, after the correction, the main sources of imprecision in the reconstruction are pixel size and imprecise 2D projections. Usually this imprecision will not result in a reconstruction error larger than 0.5 mm, which is an empirically determined value. It is therefore possible to detect incorrect matching: If for all seeds the reconstruction error remains below 0.5 mm the reconstruction can be considered as successful (see Fig. 4).

The fact that incorrect matching can be detected allows a significant improvement of the performance of the algorithm. After the first run of the algorithm it is expected that most of the projections will be correctly matched and that distortions will be corrected. Therefore, the next run of the algorithm can be done with a reduced set of projections. Usually a bad matching affects the seeds whose position along y axis is similar. Therefore projections that are included in the next matching are projections assigned to seeds whose reconstruction error is larger than 0.5 mm. If $\mathbf{p}_{ij}$ is such projection we include all projections $\mathbf{p}_{kj}$ that satisfy

$$|y_{kj}-y_{ij}|<\delta, \tag{14}$$

where $\delta=1$ mm is an empirically determined value. The results presented in Sec. VII are obtained with this modification of the algorithm.

VII. RESULTS

First, the results obtained with the algorithm we proposed is illustrated on two clinical cases for which the three-film method failed. In the first example, the three-film method failed because of an angular error of 10° (two films taken at 320° and 330° were accidentally swapped). Projections of reconstructed seeds without correction are shown on Fig. 3.

Clearly, using a fixed threshold it would be impossible to reconstruct this implant since the seeds are not equally affected by rotation. Even for perfect matching for some seeds the reconstruction error is larger than 2 mm. Our new algorithm correctly matched and reconstructed the implant. The angular error of 10° was correctly detected. Projections of the reconstructed seeds with correction are shown in Fig. 3.

The second example illustrates the ambiguities created by specific configurations of seeds, for one of clinical cases, Fig. 5. The three-film method found a solution such that all reconstruction errors are smaller than 2 mm. This solution is incorrect and a better solution is found with the proposed algorithm.

Even if the difference between the two sets of projections seems to be small, the effect of this difference in 3D space is quite dramatic, resulting in a largest displacement of 11 mm, which is an unacceptable error, as shown in Fig. 5.

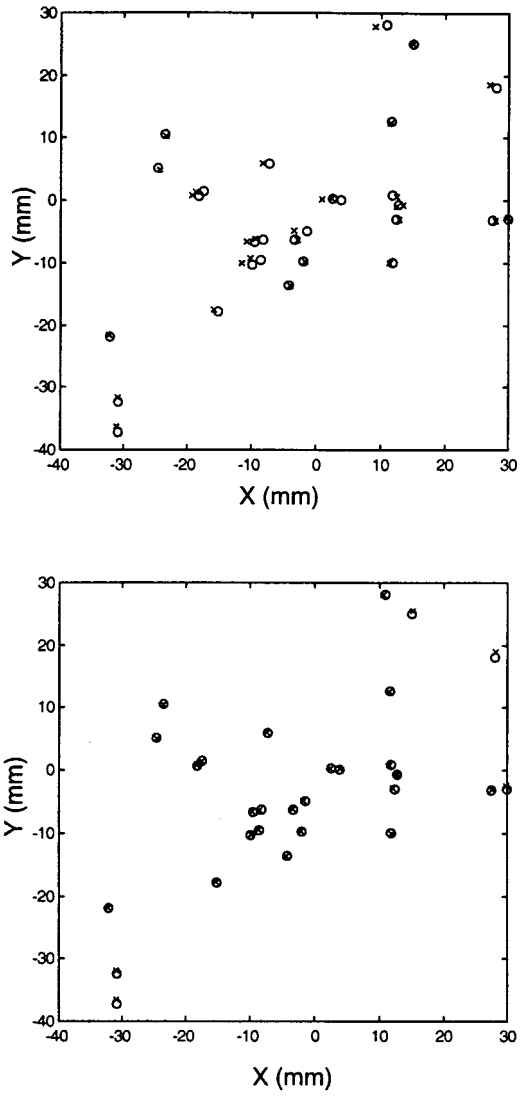

FIG. 3. Correction of the distortions: backprojected seeds without the correction (top), backprojected seeds after the correction of distortions (bottom). The open circles stand for the original projections while the crosses are projections of the reconstructed seeds. The $X-Y$ plane represents the projection of the seeds from looking down at the patient with X being the left–right axis and Y the implant axis.

The validation of the reconstruction can also be illustrated in the example shown in Figs. 4 and 5: Seeds that have been incorrectly matched have a reconstruction error larger than 0.5 mm (circled projections) and those seeds were detected using the criteria defined in Eq. (14). Note that the validation is possible only if the distortions have already been corrected.

The algorithm has been tested on two sets of implants. The first set contains 100 implants whose seed positions were generated by computer. The second set contains 112 clinical implants.

In order to simulate distortions, for simulated implants, implants were both translated and rotated before the seeds were projected, and each projection was translated separately. The conditions of the test are summarized as follows:

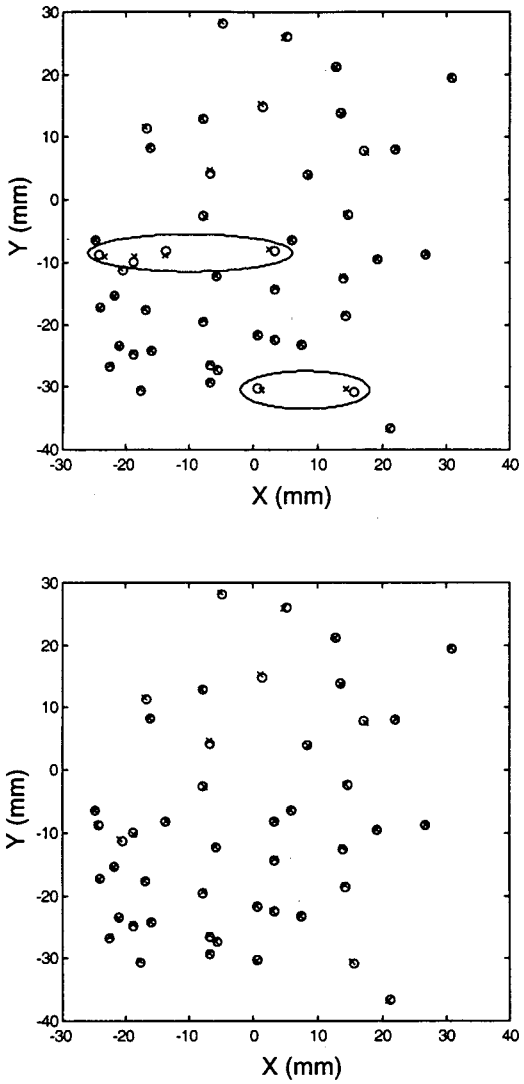

FIG. 4. Illustration of the effect of the wrong matching: backprojected seeds in case of the wrong matching (top), backprojected seeds with correctly matched projections (bottom). Incorrectly matched projections are circled. The open circles stand for the original projections while the crosses are projections of the reconstructed seeds. The $X-Y$ plane represents the projection of the seeds from looking down at the patient with X being, the left–right axis and Y the implant axis.

(1) number of seeds randomly chosen from the interval [40,70];
(2) all seeds are inside a cube whose dimensions are $4\times4\times4$ cm;
(3) seeds have been rotated around all three axes—rotation angles are randomly selected from the interval $[-2.5°, 2.5°]$;
(4) all seeds are translated during each ''acquisition'' for at most 5 mm;
(5) all projections are translated separately in random directions for at most 0.5 mm;
(6) All random values had uniform distribution.

The results are shown on histograms in Fig. 6.

For the simulated implants the distance between the reconstructed and exact positions of seeds was measured. For

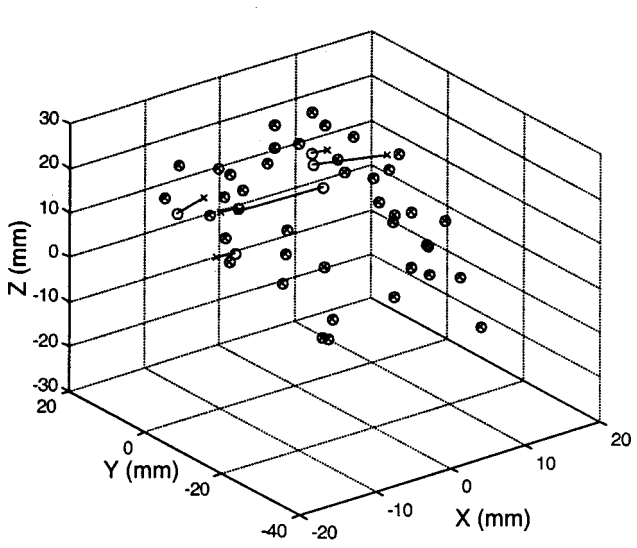

FIG. 5. The effect of the wrong matching. The open circles represent the seeds reconstructed with incorrectly matched projections. The crosses are the seeds reconstructed with correctly matched projections. X is the left–right axis, Y is the implant axis, and Z is AP axis.

all 100 implants, the average distance was 0.21 mm, the average maximal distance is 1.1123 mm, and the maximal distance is 2.4557 mm. The maximal distance was greater than 2 mm for three implants only, for one or two seeds in each implant.

We also reconstructed implants for 112 patients and compared the results with the results previously obtained using the three-film method. For the clinical cases, of course, it is not possible to measure the precision since the seed positions are not known in advance, but it is possible to measure the relative performance by comparing the results with the results previously obtained by three-film method. Since the distortions were not corrected during the reconstruction using the three-film method, the new algorithm always gives better results. In order to make a fair comparison, only the matching produced by the three-film method is used.

The seed positions were reconstructed under same conditions for both methods including the correction for distortions. As a measure of the performance both maximum (E_M) and average (E_m) reconstruction error were considered. Clearly the method that gives both smaller average and maximum errors results in a better approximation of the original implant. The number of seeds in these implants ranges from 30 up to 97.

Even if the new algorithm gives smaller error in 64% of the cases it does not always result in large difference between the two seed clouds. However, for some cases, the difference is as large as 2 cm. For example in Fig. 5 the largest distance was 1.17 cm.

For 16 patients, the three-film method completely failed, giving unacceptable error (larger than 2 mm), and those results were not recorded. The new algorithm successfully reconstructed the implants for these 16 patients. For the other 96 patients the results are shown in Figs. 7 and 8.

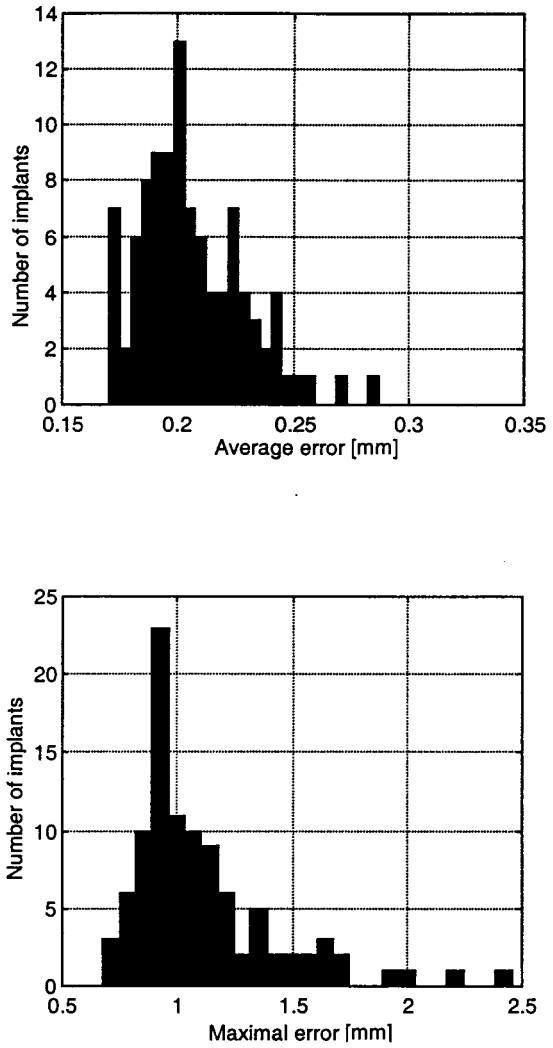

FIG. 6. Average error distribution (top) and maximum error distribution (bottom).

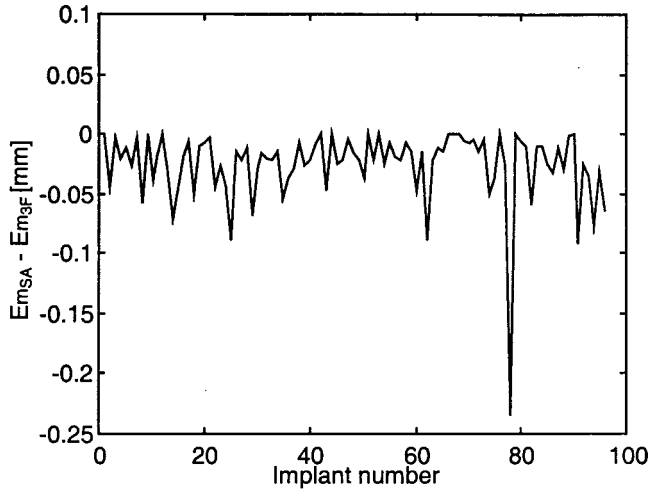

FIG. 7. The difference between the average errors for 96 clinical patients. $E_{m_{SA}}$ represents the average reconstruction error of the new method, and $E_{m_{3F}}$ is the average reconstruction error of the three-films method

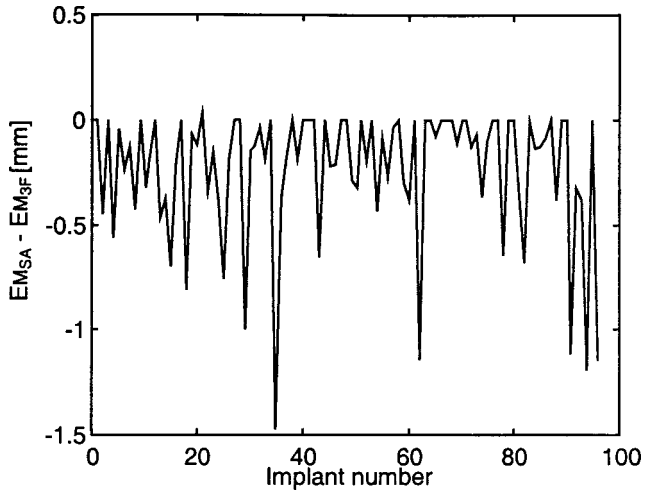

FIG. 8. The difference between the maximum reconstruction errors for 96 clinical patients. The average reconstruction error of the new method is given by $E_{M_{SA}}$, while $E_{M_{3F}}$ gives the average reconstruction error of the three-films method.

For 62 patients, the maximum errors were smaller for the reconstruction using the new algorithm, and for 83 patients, the average errors were smaller than the average error of the three-film method. The average and maximum errors for 112 implants obtained with the new method are shown in Fig. 9.

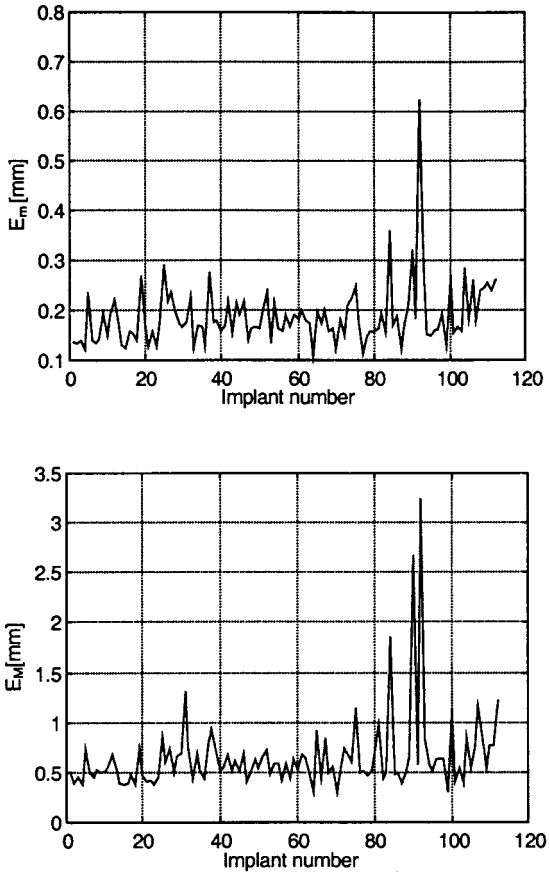

FIG. 9. Average (top) and maximum (bottom) reconstruction errors for all 112 clinical cases.

For three patients the maximum error is larger than 1.5 mm and the average error is larger than 0.3 mm. In these cases, the reconstruction is considered as having failed. The reason for this was found to be limited to incorrect extraction of 2D projections due to a very low contrast on the films.

As a validation criteria a maximum error threshold of 0.5 mm was established. There are two reasons why the maximum error goes beyond that value. In some cases only a few projections were incorrectly marked (usually 1–3 seeds). For the rest of the implants the projections seem to be scaled along the *y* axis, which is probably caused by an improper position of the film. This problem has not occurred with fluoroscopic images.

The execution time of the algorithm depends on the level of distortions and the number of seeds. For the 112 clinical cases for which the reconstruction was performed, the execution time, on average, was 1 min. Correction is performed typically in less than 5 s. Note that, in some cases, the algorithm iterated up to 5 times before the reconstruction was accepted. In those cases the execution time is larger. Usually, just one iteration suffices. All the results were obtained using an IBM PC compatible computer with Pentium III processor running on 733 MHz.

VIII. CONCLUSION

A novel algorithm for 3D prostate implant reconstruction has been presented. The algorithm offers completely automatic correction of distortions, matching, and validation of the reconstruction.

When compared with the three-film method, the new method gives an improvement in 62% of the cases. The three-film method can successfully reconstruct about 86% implants while the new method gives correct reconstruction in 100% of the cases, provided that the projections are correctly identified on the images. The new method also offers an advantage of providing an automatic correction of the distortions. Without the correction, the operator has to correct the distortions manually, which can be extremely difficult and can take several hours. A comparison of the required times for the reconstruction for the new and the three-film method is summarized in Table II.

The algorithm was validated on 112 clinical cases as well as on 100 implants generated by computer. The results of the reconstruction and a comparison with three-film method were also presented. The algorithms presented in this paper were implemented in C++ and are in regular clinical use at our institution.

TABLE II. Clinical comparison of the workload for the new method and the three-films method.

	New method (fluo)	Three-film method
Patient positioning	10–15 min	10–15 min
Acquisition of images (and film development)	2 min	20–30 min
Identification of seeds	1–15 min	30 min–1 h
Matching and correction	1–5 min	1 h or more
Total	14–40 min	2 h or more

ACKNOWLEDGMENTS

This work has been supported in part by The National Cancer Institute of Canada with funds from the Canadian Cancer Society, by Fonds pour les Chercheurs(es) et l'Aide à la Recherche (FCAR) of province of Québec, and National Science and Engineering Research Council of Canada (NSERC).

[1] H. I. Almos and I. I. Rosen, "A three film technique for reconstruction of radioactive seed implants," Med. Phys. **8**, 210–214 (1981).
[2] M. D. Altschuler, P. A. Findlay, and R. D. Epperson, "Rapid, accurate, three-dimensional location of multiple seeds in implant radiotherapy treatment planning," Phys. Med. Biol. **28**, 1305–1318 (1983).
[3] P. J. Biggs and D. M. Kelley, "Geometric reconstruction of seed implants using a three-film technique," Med. Phys. **10**, 701–704 (1983).
[4] M. S. Rosenthal and R. Nath, "An automatic seed identification technique for interstitial implants using three isocentric radiographs," Med. Phys. **10**, 475–479 (1983).
[5] D. H. Brinkmann and R. W. Kline, "Automated seed localisation from CT datasets of the prostate," Med. Phys. **25**, 1667–1672 (1998).
[6] J. N. Roy, K. E. Wallner, P. J. Harrington, C. C. Ling, and L. L. Anderson, "A CT-based evaluation method for permanent implants: Application to prostate," Int. J. Radiat. Oncol., Biol., Phys. **26**, 163–169 (1993).
[7] W. S. Bice, D. F. Dubois, J. J. Prete, and B. R. Prestidge, "Source localization from axial image sets by iterative relaxation of the nearest neighbor criterion," Med. Phys. **26**, 1919–1924 (1999).
[8] E. Aarts and J. Korst, *Simulated Annealing and Boltzmann Machines* (Wiley, New York, 1989).
[9] S. Kirkpatrick, C. D. Gellat, Jr., and M. P. Vecchi, "Optimisation by simulated annealing," Science **220**, 671–680 (1982).
[10] M. Matsumoto and T. Nishimura, "Mersenne Twister: A 623-dimensionally equidistributed uniform pseudorandom number generator," ACM Trans. Model. Comput. Simul. **8**, 3–30 (1998).
[11] R. P. Brent, *Algorithms for Minimization Without Derivatives* (Prentice–Hall, Englewood Cliffs, NJ, 1973).